Check for updates

ARTICLE

Essential role of P-glycoprotein in the mechanism of action of oliceridine

Emilya Ventriglia[1], Arianna Rizzo[2,3], Juan L. Gomez[1], Jacob Friedman[4,5], Sherry Lam[1], Oscar Solís[1], Rana Rais[5,6,7], Jordi Bonaventura[1,2,3✉] and Michael Michaelides[1,8✉]

Mu opioid receptor (MOR) agonists comprise the most effective analgesics, but their therapeutic utility is limited by adverse effects. One approach for limiting such effects has been to develop "biased" MOR agonists that show preference for activating G protein over β-Arrestin signaling. However, the notion of biased agonism has been challenged by recent studies. Oliceridine (Olinvyk®, TRV-130, OLC) is a selective MOR agonist approved by the FDA in 2020 for pain management in controlled clinical settings. Oliceridine purportedly demonstrates diminished adverse effects compared to morphine or other MOR agonists, a profile attributed to its biased agonism. However, recent studies suggest that oliceridine does not display biased agonism but instead weak intrinsic efficacy for G protein and β-Arrestin activation. Nevertheless, these insights have been derived from in vitro studies. To better understand oliceridine's in vivo efficacy profile, we performed a comprehensive assessment of its in vitro and in vivo pharmacology using both cultured cells and rodents. In vitro, oliceridine displayed high MOR affinity and weak intrinsic efficacy. In vivo, oliceridine showed impaired brain penetrance and rapid clearance, effects we attributed to its interaction with the P-glycoprotein (P-gp) efflux transporter. Moreover, we found that P-gp was essential for oliceridine's in vivo efficacy and adverse effect profiles. Taken together with prior studies, our results suggest that oliceridine's in vivo efficacy and adverse effect profiles are not attributed solely to its weak intrinsic efficacy or biased agonism but, to a large extent, its interaction with P-gp as well.

INTRODUCTION

The Mu opioid receptor (MOR) is a G protein-coupled receptor expressed widely throughout the body but most notably in brain regions involved in nociception, respiration, and reinforcement. MOR agonists are the most potent and efficacious analgesics available for treatment of moderate to severe acute pain. Despite this, their therapeutic window is constrained by adverse effects, including constipation, respiratory depression, tolerance, and abuse liability. To reduce such effects, research efforts have focused on developing MOR agonists capable of eliciting analgesia with reduced adverse effects. One major area of research involves MOR functional selectivity and the development of "biased" MOR agonists which differ in their recruitment of G proteins vs. β-Arrestins [1].

Early studies that characterized functional outcomes across different effector pathways suggested that opioid analgesia is mediated by G protein-dependent signaling and that adverse effects are mediated by β-Arrestin-triggered pathways. In particular, it was shown that mice with germline deletion of β-Arrestin2 exhibit enhanced morphine-induced thermal antinociception with diminished respiratory depression, constipation, and

antinociceptive tolerance [2–4]. Thus, several novel G protein-biased agonists have been developed, including PZM21, SR-17018, and oliceridine [5]. However, recent studies examining β-Arrestin2 signaling as well as G protein-dependent mechanisms of MOR-dependent respiratory depression have failed to support this dichotomy [6]. Specifically, several recent studies have been unable to independently reproduce the effects of global β-Arrestin2 gene deletion [7, 8] or impaired MOR-dependent β-Arrestin2 signaling [9] on opioid-induced respiratory depression, constipation, or tolerance.

Evidence suggests that the novel MOR selective "biased" agonist oliceridine, which was granted FDA approval in 2020 for pain management in controlled clinical settings, may exhibit a reduction in MOR-induced adverse effects while maintaining potent analgesia [5]. Oliceridine is the first G protein-biased MOR agonist approved for clinical use, yet its therapeutic potential remains to be fully demonstrated. Early preclinical studies using oliceridine in rodents reported improved therapeutic potential compared to morphine, demonstrating reduced respiratory depression and constipation at equianalgesic doses [5]. However, clinical data for oliceridine are less clear, with patients

[1]Biobehavioral Imaging and Molecular Neuropsychopharmacology Unit, National Institute on Drug Abuse, Baltimore, MD 21224, USA. [2]Departament de Patologia i Terapèutica Experimental, Institute de Neurociències, Universitat de Barcelona, L'Hospitalet de Llobregat, Catalonia, Spain. [3]Neuropharmacology & Pain Group, Neuroscience Program, Bellvitge Institute for Biomedical Research (IDIBELL), L'Hospitalet de Llobregat, Catalonia, Spain. [4]Medications Development Program, Molecular Targets and Medication Discovery Branch, National Institute on Drug Abuse, Baltimore, MD 21224, USA. [5]Johns Hopkins Drug Discovery, Johns Hopkins School of Medicine, Baltimore, MD 21205, USA. [6]Department of Neurology, Johns Hopkins School of Medicine, Baltimore, MD 21205, USA. [7]Department of Pharmacology, Johns Hopkins School of Medicine, Baltimore, MD 21205, USA. [8]Department of Psychiatry and Behavioral Sciences, Johns Hopkins School of Medicine, Baltimore, MD 21205, USA. ✉email: jbonaventura@ub.edu; mike.michaelides@nih.gov

experiencing a similar adverse effect profile at equipotent doses to morphine, thus the therapeutic widening oliceridine demonstrates in humans appears modest [10, 11]. Similarly, preclinical studies in rodents have shown that oliceridine, like other MOR agonists, elicits respiratory depression, constipation, antinociceptive tolerance, and abuse-related behaviors [12–17].

An alternative hypothesis that may explain the discrepancies in therapeutic window across opioids involves the G protein activation efficacy of such ligands. Specifically, a recent study showed that oliceridine does not exhibit "bias" per se, but weak intrinsic efficacy [13]. This finding suggests that MOR biased agonism is not necessarily involved in oliceridine's purported improved safety profile. However, these insights were mostly derived from the use of heterologous receptor expression in cell culture which does not fully recapitulate the complex and dynamic processes a drug encounters upon systemic in vivo exposure. Furthermore, the in vivo features of oliceridine and its mechanism of action have not been thoroughly characterized. To address these shortcomings, we performed in vitro and in vivo studies of oliceridine in cell culture, mice, and rats.

MATERIALS AND METHODS
Animal subjects
Male mice (C57BL/6 J, 20–25 g) were ordered from Jackson Laboratory and maintained under a normal 12-h light/dark cycle with food and water freely available. Mdr1a/b knockout (KO) mice (FVB.129P2-Abcb1a^{tm1Bor}-Abcb1b^{tm1Bor} N12) and FVB background wild-type (WT) controls were ordered from Taconic. Male and female Sprague-Dawley rats (strain code #400, 200–250 g) were ordered from Charles River. Mdr1a/BCRP KO rats (hsdsage: SD-Mdr1a^{tm1sage}-Abcg2^{tm1sage}) were ordered from Envigo. Rats were maintained under a reverse 12-h light/dark cycle with ad libitum food and water throughout all experiments. Experiments and procedures complied with ethical regulations for animal testing and research, followed the NIH guidelines and were approved by the NIDA animal care and use committee. The experimenters were blinded to the group allocation.

Radioligand binding assays
Brain tissue lacking cerebellum was suspended in Tris-HCl 50 mM pH 7.4 buffer supplemented with protease inhibitor cocktail ((Sigma) 1:1000) and disrupted with a Polytron homogenizer (Kinematica, Basel, Switzerland). Homogenates were centrifuged at 48,000 g (50 min, 4 °C) and washed 2 times to isolate the membrane fraction. For hMOR CHO-K1 cell membranes (Perkin Elmer), tissue was suspended in 50 mM Tris-HCl pH 7.4. Protein was quantified by the bicinchoninic acid method (Pierce).

Saturation binding. Membrane suspensions (50 μg of protein/mL) were incubated in 50 mM Tris-HCl (pH 7.4) containing 10 mM MgCl$_2$ and increasing concentrations of [^{3}H]oliceridine (79 Ci/mmol, Novandi Chemistry AB) during 2 h (Rat) or 1 h (hMOR) at RT.

Competition binding. Membrane suspensions (50 μg of protein/mL) were incubated in 50 mM Tris-HCl (pH 7.4) containing 10 mM MgCl$_2$, either 2.5 nM of [^{3}H]DAMGO (44-48 Ci/mmol, PolyPeptide Labs, San Diego, CA) or 1.6 nM [^{3}H]oliceridine and increasing concentrations of competing ligand during 1–2 h at RT.

In all cases, non-specific binding was determined using naloxone (10 μM) and free and membrane-bound radioligand were separated by rapid filtration in 96-well GF/B filter plates (presoaked in 0.5% BSA) and washed with 9 × 500 μl of ice-cold Tris-HCl buffer. Radioactivity was measured using a Microbeta2 plate counter (Perkin Elmer, Boston, MA, USA) (41% efficiency). One-site competition curves were fitted using Prism 9 (Graphpad Software, La Jolla, CA, USA). Ki values were calculated using the Cheng-Prusoff equation.

In vitro functional assays
HEK-293T cells (ATCC) were maintained in Dulbecco's modified Eagle medium (DMEM; Sigma-Aldrich, Saint Louis, MO) supplemented with 100 U/ml penicillin (Biowest, Nuaillé, France), 100 mg/ml streptomycin (Biowest), 10% v/v heat-inactivated fetal bovine serum (Invitrogen, Carlsbad, CA, USA), non-essential amino acids (Biowest), 100 mM sodium pyruvate

(Biowest) and 2 mM L-glutamine (Biowest) and kept in an incubator at 37 °C and 5% CO$_2$.

cAMP. Cells were seeded on 100 mm dishes at 2.2×10^6 cells/dish 24 h before transfection and transfected with 10 μg cDNA encoding human MOR, KOR or DOR and 10 μg of cDNA encoding for the R-FlincA biosensor using polyethylenimine (PEI; Polysciences Europe GmbH)) in a 1:3 DNA:PEI ratio. Cells were harvested 48 h after transfection. cAMP accumulation was measured using the R-FlincA (Red Fluorescent indicator for cAMP) biosensor [18]. On experiment day, cells were harvested, washed in PBS pH 7.4 and resuspended in PBS containing 5.6 mM glucose and 0.5 U/ml of Adenosine Deaminase (Roche). Cells were then plated in 96-well black flat bottom plates and fluorescence was measured using a CLARIOstar (BMG Labtech) plate reader with excitation at 550 nm and emission at 600–640 nm to establish their baseline fluorescence (F$_0$). Cells were then incubated with increasing amounts of oliceridine or morphine and forskolin (5 μM) for 10 min and their fluorescence was measured again (F). Relative fluorescence changes were obtained by calculating the fluorescence ratio before and after treatment (F/F$_0$). cAMP inhibition was expressed as % morphine maximum response and concentration-response curves were fitted using Prism 9.

β-arrestin recruitment. HEK-293T cells were seeded on 6-well culture plates at 3×10^6 cells/well and grown in DMEM (Thermo Fisher) supplemented with L-Glutamine 200 mM, Sodium Pyruvate 100 mM, MEM non-Essential Amino Acids (Biowest), 10% fetal bovine serum (FBS; Merck KgaA), streptomycin (100 μg/mL), and penicillin (100 μg/mL) in a controlled environment (37 °C, 98% humidity, 5% CO$_2$). 24 h after seeding, cells were transfected with split NanoBiT® vectors NB MCS1 (Promega, Madison, WI, United States) fused to β-arrestin2 or hMOR (0.1 μg β-arrestin2 LgBIT cDNA, 2 μg of the hMOR-SmBIT cDNA) using PEI (Polysciences Europe GmbH) in a 1:3 DNA:PEI ratio. 48 h after transfection, cells were rinsed, harvested, and resuspended in 4 mL/well of Hanks' Balanced Salt solution (HBSS, Sigma Aldrich). Cells (80 μl/well) were then plated in 96-well white plates (PO-204003, BIOGEN) and immediately treated with increasing concentrations of DAMGO, morphine or oliceridine, 5 min later 2 μM coelenterazine (Prolume Ltd) was added and luminescence (490 to 410 nm) was measured during 6 min using a CLARIOstar plate reader. β-arrestin recruitment was expressed as % of DAMGO maximum effect and concentration-response curves were fitted using Prism 9.

[^{35}S]GTPγS Recruitment
The procedure was performed with slight modifications to previously published protocols [19]. Membranes were preincubated for 30 min at room temperature in 50 mM Tris-HCl (pH 7.4), 1 mM EDTA, 100 mM NaCl, 5 mM MgCl$_2$, 10 μM GDP and DPCPX 1 μM. The reaction was initiated by adding membrane preparation (0.05 mg /mL) to incubation tubes containing drug dilutions and binding cocktail. The final concentrations were 50 mM Tris-HCl (pH 7.4), 1 mM EDTA, 100 mM NaCl, 5 mM MgCl$_2$, 0.5% BSA, 10 μM GDP, DPCPX 1 μM and 150 pM [^{35}S]GTPγS (1250 Ci/mmol, Perkin Elmer). Non-specific binding was defined using 10 μM GTPγS. Reaction tubes were incubated for 90 min at 25 °C under constant shaking. The reaction was quickly terminated by rapid filtration through 96-well GF/B filter plates (Perkin Elmer) and two additional 2 mL washes with the ice-cold buffer. Radioactivity in plates was counted as described above. Concentration-response curves were fitted using Prism 9.

[^{35}S]GTPγS autoradiography
Frozen rat brain tissue (n = 2 M/4 F) was sectioned (20 μM) on a cryostat (Leica) and thaw mounted on glass slides. Preincubation buffer was pipetted onto each slide and incubated for 20 min at RT (50 mM Tris-HCl, 1 mM EDTA, 5 mM MgCl$_2$ and 100 mM NaCl). The buffer was removed via aspiration and incubated for 60 min in pre-incubation buffer containing 2.7 mM GDP and 1.3 μM DPCPX. GDP buffer was removed and [^{35}S]GTPγS cocktail (GDP buffer, 20 mM DTT, 300 nm [^{35}S]GTPγS) with agonists of interest (oliceridine 10 μM; DAMGO 10 μM), without agonists (basal condition), or with a saturated concentration of non-radioactive GTP (for non-specific binding) was pipetted onto each slide and incubated for 90 min. For antagonist cotreatment, slides were incubated with GDP buffer containing naloxone (1 μM) for 60 min before addition of [^{35}S]GTPγS and agonist cocktail. The [^{35}S]GTPγS cocktail was removed via aspiration and slides were washed in ice cold buffer (50 mM Tris-HCl, 5 mM MgCl$_2$, pH 7.4) for 5 min (2x) followed by a 30 sec dip in ice cold water. Slides were apposed to a BAS-SR2040 phosphor screen (Fujifilm)

for 3 days and imaged using a phosphorimager (Typhoon FLA 7000; GE Healthcare).

[³H]Oliceridine and [³H]DAMGO autoradiography
Frozen tissue was sectioned (20 µM) on a cryostat (Leica, Germany) and thaw mounted onto Superfrost Plus glass slides (Avantor, USA). Following incubation, slides were air dried and apposed to a BAS-TR2025 Phosphor Screen (Fujifilm) for 5–10 days and imaged using a phosphorimager (Typhoon FLA 7000).

In vivo uptake. For rat [³H]oliceridine uptake, rats were injected with [³H] oliceridine (1 µCi/g, i.v.) with or without naloxone pretreatment 5 min before (10 mg/kg, s.c.) and euthanized 15 min following [³H]oliceridine administration. For efflux transporter inhibitor cotreatment uptake studies, rats were co-injected with either MK571 (1 mg/kg) or Tariquidar (1 mg/kg) alongside [³H]oliceridine (1 µCi/g, i.v.) and euthanized 15 min later. For WT mouse uptake, [³H]oliceridine (10µCi/g, i.p.) was administered 15 min prior to euthanasia. For BCRP KO and P-gp KO mouse uptake, mice were injected with [³H]oliceridine (10 µCi/g, i.p.) and euthanized 15 min later.

In vitro autoradiography. Slides were pre-incubated (10 min, RT) in incubation buffer (50 mM Tris-HCl, 10 mM MgCl₂, pH 7.4), then incubated (60 min, RT) in incubation buffer containing [³H]oliceridine or [³H]DAMGO. Non-specific binding was determined in the presence of 10 µM naloxone.

Ex vivo occupancy. Rats were injected with oliceridine (1 mg/kg/s.c.), naloxone (1 mg/kg,s.c.), or saline. Brains were harvested 15-, 30-, or 60-min post-injection. Brain slices were incubated 10 min in buffer (50 mM Tris-HCL, 10 mM MgCl₂) containing [³H]oliceridine (5 nM).

Efflux transporter panel
These experiments were performed by an outside vendor (Eurofins, France). Oliceridine was tested in P-gp substrate assessment assays at 10 µM. The A to B and B to A permeability was measured in CaCo-2 cells in the presence and absence of verapamil, a P-gp inhibitor. Efflux ratios (E) were calculated based on the apparent B–A and A–B permeability with and without verapamil. In each experiment, the respective reference compound was tested concurrently with the test compound to assess the assay reliability. Fluorescein was used as the cell monolayer integrity marker. Fluorescein permeability assessment (in the A–B direction at pH 7.4 on both sides) was performed after the permeability assay for the test compound. The cell monolayer that had a fluorescein permeability of less than $1.5 \times 10{-}6$ cm s $-$ 1 for CaCo-2 was considered intact, and the permeability result of the test compound from intact cell monolayer was reported.

Metabolite identification
Metabolite identification (MET-ID) was performed on a Dionex ultra high-performance LC system coupled with Q Exactive Focus orbitrap mass spectrometer (Thermo Fisher Scientific Inc., Waltham MA). Separation was achieved using Agilent Eclipse Plus column (100 × 2.1 mm i.d; maintained at 35oc) packed with a 1.8 µM C18 stationary phase. The mobile phase consisted of 0.1% formic acid in water and 0.1% formic acid in acetonitrile. Pumps were operated at a flow rate of 0.3 ml/min for 7 min using gradient elution. The mass spectrometer controlled by Xcalibur software 4.0.27.13 (Thermo Scientific) was operated with a HESI ion source in positive ionization mode. Metabolites were identified in the full-scan mode (from m/z 50 to 1600) by comparing t = 0 samples with t = 60 min samples and structures were proposed based on the accurate mass information.

Hot plate
The procedure is based on the design of a previous study [20]. Opioid-induced thermal antinociception was measured using a hot plate apparatus (52.5 °C; Ugo Basile). Rats were previously habituated to the apparatus. For testing, rats were placed on the hot plate within a plexiglass cylinder and observed for latency of presentation of signs of nociception (i.e., withdrawal/licking of hind paw or jumping). A 30 sec cutoff was used to prevent tissue damage. Experimenter was blinded to all drug conditions. Rats received morphine (10 mg/kg, s.c.) or oliceridine (0.3 mg/kg, s.c.) and their withdrawal latency measured in a similar time course. The percentage of the maximum possible effect is calculated as: %MPE = (latency^{drug} – latency^{baseline})/(cutoff – latency^{baseline}) × 100. Baseline latency was determined for each subject 15 min prior to drug.

Pulse oximetry
Oxygen Saturation was measured in freely moving rats using a collar sensor and pulse oximetry (MouseOx Plus, Starr Life Sciences). Animals were habituated to experimenter handling and wearing oximeter collars daily for 2 weeks prior to testing. After baseline readings, rats (n = 4–6 male and 6 female per group) received morphine (10 mg/kg, s.c.) or oliceridine (0.3 mg/kg, s.c.), followed by repeated oximetry readings (0–240 min). Oximetry readings were averaged across a 60 sec period for the respective time points. Experimenter was blinded to all drug conditions.

Self-administration
The procedure was based on previous studies [21, 22] in non-food restricted rats. Detailed methods are described in the supplementary materials.

RESULTS
Oliceridine binds MOR with high affinity but does not stimulate [³⁵S]GTPγS recruitment in brain tissue
Prior studies reported a detailed in vitro characterization of oliceridine [5, 13, 23–27]. However, the vast majority of these data were derived from experiments using transfected cells. Whereas experiments in cell culture can provide important molecular insights into the functional selectivity profile of a drug, they rely on overexpression of the target receptor in an artificial environment. Thus, their ability to emulate all physiologically relevant expression patterns and conditions is limited [28, 29]. To extend these findings to a more physiologically relevant model, we assessed oliceridine's ability to displace [³H]DAMGO in rat brain membranes using competitive radioligand binding assays. Consistent with prior findings [23, 27], oliceridine exhibited a Ki of 1.6 ± 0.2 nM for MOR and no sex-dependent differences were observed (Fig. 1A).

Next, we performed agonist-stimulated [³⁵S]GTPγS recruitment assays using rat brain membranes. In contrast to DAMGO, which led to a significant and concentration-dependent increase in [³⁵S] GTPγS recruitment, oliceridine did not (Fig. 1B). There was no difference in [³⁵S]GTPγS recruitment as a function of sex. To rule out that the oliceridine-dependent signal might have been weak due to dilution of MOR density in the whole-brain membrane preparation and oliceridine's known low intrinsic efficacy, we examined whether oliceridine increased [³⁵S]GTPγS recruitment in situ using [³⁵S]GTPγS autoradiography (n = 2 M/4 F rats). DAMGO (10 µM) led to a significant increase in [³⁵S]GTPγS recruitment in brain regions with MOR expression: caudate putamen; CPu ($p < 0.001$), nucleus accumbens; NAc ($p < 0.001$), and prefrontal cortex; PFC ($p < 0.001$). In contrast, oliceridine (10 µM) did not (Fig. 1C, D).

Next, we tested whether oliceridine inhibited cAMP accumulation in HEK293 cells expressing hMOR, hDOR or hKOR. Oliceridine was a potent partial agonist at hMOR (EC50 0.41 ± 0.25 nM, Emax 50.1 ± 2.7) and a weak full agonist at hKOR (EC50 79 ± 6 nM, Emax 89 ± 3) but was inactive at hDOR (Fig. 1F–H). Similar to previous reports, oliceridine exhibited little to no signal in β-arrestin recruitment relative to DAMGO, while morphine-induced β-arrestin recruitment was ~50% of DAMGO (Fig. 1E).

[³H]oliceridine characterization
The complex processes that a drug is subjected to in vivo cannot be easily mimicked using in vitro experiments, so we synthesized [³H]oliceridine (Fig. 2A) for studying oliceridine's in vivo properties. To validate [³H]oliceridine, we performed saturation and competition binding assays in rat brain membranes and in membranes from CHO-K1 cells transfected with hMOR. [³H]oliceridine showed specific binding with high affinity in rat brain (Kd = 0.9 ± 0.2 nM, Bmax = 0.13 ± 0.01 pmol/mg of protein) (Fig. 2B) and at hMOR (Kd = 0.9 ± 0.9 nM, Bmax = 9.9 ± 2.7 pmol/mg of protein) (Fig. 2D).
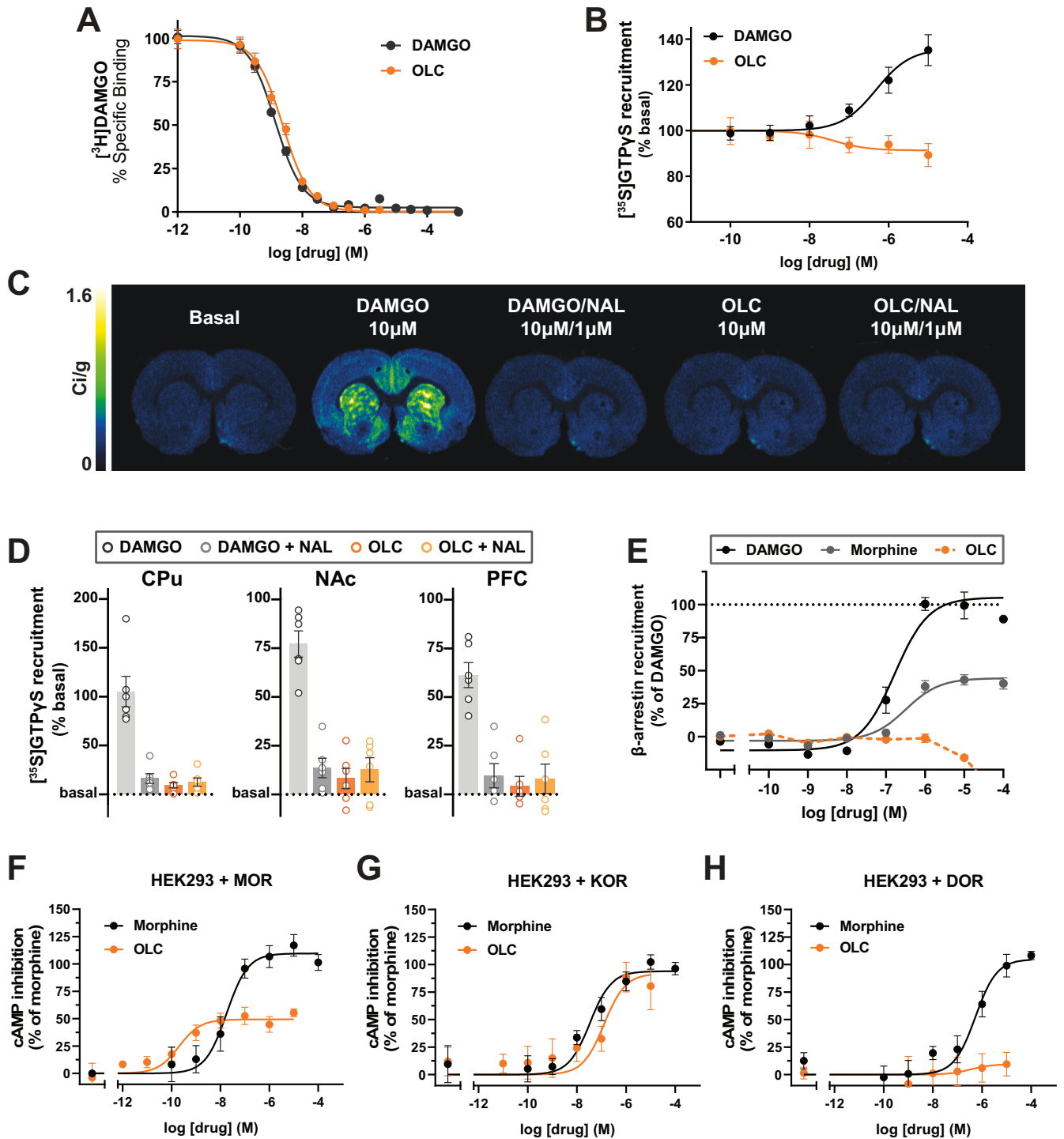
Fig. 1 Oliceridine binds MOR with high affinity but does not stimulate [35 S]GTPγS recruitment in brain tissue. A [³H]DAMGO (MOR) specific binding to rat brain membranes against increasing concentrations of DAMGO (black) or oliceridine (orange). **B** [³⁵S]GTPγS recruitment in rat brain membranes using increasing concentrations of either DAMGO (black) or oliceridine (orange). All data points are mean ± SEM of representative experiments performed in triplicate (experiments were performed 3 to 6 times to estimate the parameters) with Ki, EC50 and Emax reported in the main text. **C** [³⁵S]GTPγS autoradiography in rat brain sections treated with saline, DAMGO (10 μM), or oliceridine (10 μM) with or without naloxone (1 μM). **D** Quantification of autoradiography images: caudate putamen (CPu), nucleus accumbens (NAc), prefrontal cortex (PFC). Data points represent average of 4–6 sections per animal ($n = 2$ M, 4 F rats/condition). %Binding = 100-[(group mean)/saline group mean)]*100. **E** β-Arrestin assay performed in HEK-293 cells transiently transfected with hMOR. **F–H** In vitro cAMP signaling elicited by morphine or oliceridine in HEK-293 cells transiently transfected with (**F**) hMOR, (**G**) hKOR, and (**H**) DOR.

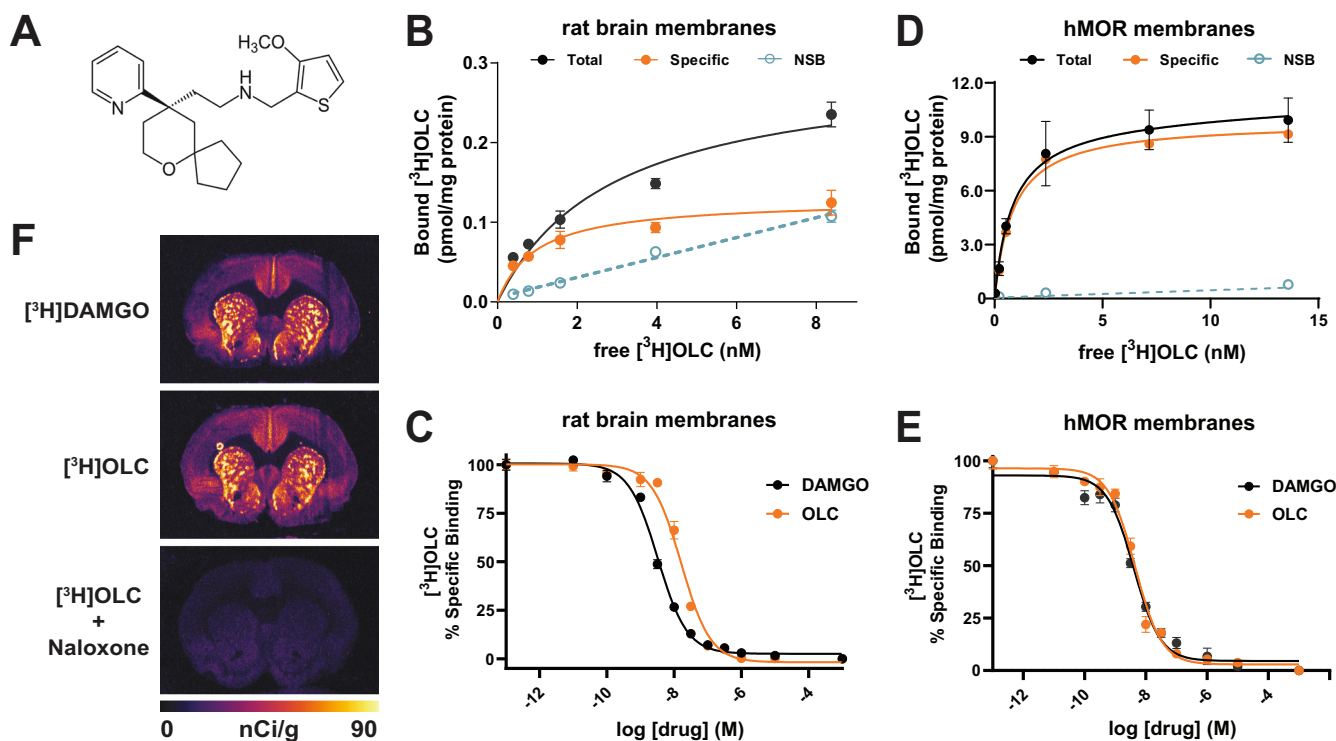**Fig. 2 Synthesis and characterization of [³H]oliceridine. A** [³H]oliceridine structure. **B** [³H]oliceridine saturation binding assay in rat brain membranes and **C** CHO-K1 cell derived membranes transfected with hMOR. [³H]oliceridine-specific binding in the presence of increasing concentrations of DAMGO (black) or oliceridine (orange) in rat brain membranes (**D**) or in CHO-K1 cell derived membranes transfected with hMOR (**E**). **F** Autoradiograms showing rat brain sections incubated with [³H]DAMGO (6.2 nM) or [³H]oliceridine (12.5 nM) with or without naloxone (10 μM).

DAMGO displaced [³H]oliceridine from rat brain (Ki = 2.4 ± 0.4 nM) (Fig. 2C) and at hMOR (Ki = 2.6 ± 0.1 nM) (Fig. 2E) with high affinity, and oliceridine also displaced [³H]oliceridine from rat brain (Ki = 2.7 ± 0.7 nM) and at hMOR (Ki = 11 ± 1 nM) (Fig. 2C, E). Finally, in vitro autoradiography using [³H]oliceridine in rat brain sections showed a specific binding distribution that was identical to that observed using [³H]DAMGO (Fig. 2F).

Oliceridine exhibits rapid MOR occupancy

To examine [³H]oliceridine's in vivo performance, we pretreated rats with saline or naloxone (10 mg/kg, s.c.) followed by [³H]oliceridine (1 μCi/g, i.v.) 5 min later. Rats were euthanized 15 min after [³H]oliceridine injection and brains were harvested and imaged using a phosphorimager. We performed similar studies in mice (5 μCi/g, i.p. or s.c.). [³H]oliceridine accumulated exclusively in the choroid plexus/ventricles in a nonspecific manner (i.e., no blockade by naloxone pretreatment) and did not show MOR-specific uptake in rats or mice (Fig. 3A–C).
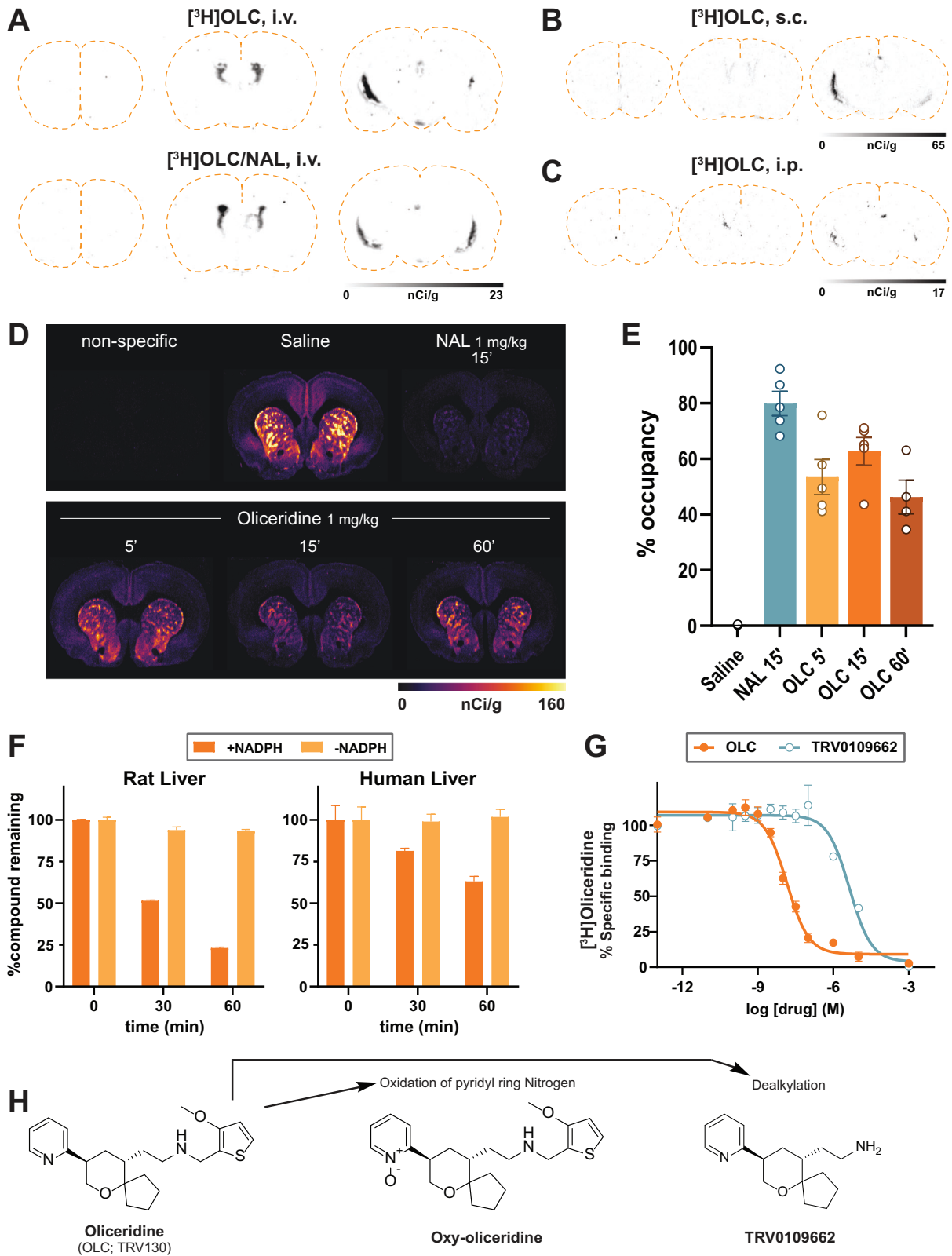
The lack of MOR binding of [³H]oliceridine in vivo given its high in vitro affinity is counterintuitive. However, [³H]oliceridine was administered at trace levels. To see if a pharmacological dose of oliceridine led to MOR occupancy in vivo, we pretreated rats with saline, naloxone (1 mg/kg, s.c.) or oliceridine (1 mg/kg, s.c.) and euthanized them at 5-, 15-, or 60-min post-injection. We then harvested and sectioned their brains and exposed the sections to a brief (10 min) incubation with [³H]oliceridine (5 nM). Naloxone led to 82.8 ± 4.1% MOR occupancy at 15 min after its injection (Fig. 3D, E). Oliceridine produced a comparable level of MOR occupancy, occupying 53.5 ± 13.9%, 67.5 ± 1.8%, and 46.3 ± 12.2% at 5-, 15, and 60-min post-injection respectively.

The difference observed between MOR occupancy at trace vs. pharmacological doses of oliceridine could be explained by conversion of [³H]oliceridine to a metabolite that lacked

radioisotopic labeling. To confirm that the MOR occupancy observed was due to oliceridine and not its metabolite, we performed metabolite identification studies in human and rat liver microsomes. In rat, the amount of oliceridine decreased by ~50% at 30 min and by ~75% at 60 min (Fig. 3F). In human liver microsomes, oliceridine showed slower metabolization, decreasing ~25% at 30 min and ~40% at 60 min (Fig. 3F). Oliceridine had two main metabolites. The major (Oxy-oliceridine, M1) was produced by oxidation of the pyridyl ring on the nitrogen and comprised ~25% of the parent in human and ~35% in rat microsomes (Fig. S1). The minor (M2, aka TRV0109662) (Fig. 3H) was produced by dealkylation and comprised ~3% of the parent in human and ~6% in rat microsomes (Fig. S1). Based on the location of the ³H, oxy-oliceridine would retain radioisotopic labeling and therefore would not be expected to contribute to any MOR occupancy. In contrast, TRV0109662 would lose the radioactive label upon metabolization from [³H]oliceridine and therefore could be involved in the MOR occupancy we observed, especially if it had higher affinity than oliceridine. To examine this, we synthesized TRV0109662 and assessed its MOR affinity. TRV0109662 exhibited a 300-fold lower affinity (Ki = 1.1 ± 0.6 μM) compared to oliceridine (Fig. 3G), ruling out its capacity as an active metabolite responsible for MOR occupancy. Collectively, these experiments rule out any meaningful contributions of oliceridine's metabolites to MOR occupancy and suggest that pharmacological doses of oliceridine produce rapid MOR occupancy in vivo.

Oliceridine's brain uptake is determined by its interaction with P-glycoprotein

The low brain uptake of [³H]oliceridine coupled with its rapid brain MOR occupancy is consistent with oliceridine's fast pharmacokinetic profile, where oliceridine plasma and brain concentrations

A [³H]OLC, i.v.

[³H]OLC/NAL, i.v.

0 nCi/g 23

B [³H]OLC, s.c.

0 nCi/g 65

C [³H]OLC, i.p.

0 nCi/g 17

D
non-specific   Saline   NAL 1 mg/kg 15'

Oliceridine 1 mg/kg
5'   15'   60'

0 nCi/g 160

E

F +NADPH -NADPH

Rat Liver   Human Liver

G OLC TRV0109662

H

Oliceridine
(OLC; TRV130)

Oxidation of pyridyl ring Nitrogen

Oxy-oliceridine

Dealkylation

TRV0109662

have been shown to peak at 5-min post injection and then steadily decline [27, 30, 31]. We hypothesized that these characteristics may be explained by oliceridine's potential interactions with efflux transporters, whose properties can prevent trace doses from accumulating in the brain but become saturated by pharmacological doses and therefore allow enough of the drug to accumulate in brain. Indeed, many opioids, including morphine, are known efflux transporter substrates [32, 33]. To examine this, we profiled oliceridine (10 µM) in its capacity to serve as a substrate for several human efflux transporters. Oliceridine was a

Fig. 3 Oliceridine exhibits rapid MOR occupancy. Autoradiograms from [³H]oliceridine ex vivo uptake experiments showing brain sections from rats (**A**) injected with [³H]oliceridine (1 µCi/g, i.v.) with or without naloxone pretreatment (10 mg/kg, s.c.), as well as mice (**D**) injected with [³H]oliceridine (10 µCi/g) subcutaneously (**B**) or intraperitoneally (**C**) and euthanized 15 min later. **D** Autoradiograms from ex vivo receptor occupancy experiments showing rat brain sections incubated with [³H]oliceridine (OLC) in rats that received either saline, naloxone (1 mg/kg, s.c., 15 min post-injection), or oliceridine i.v. (1 mg/kg, s.c 5-, 15-, or 60-min post-injection). **E** Quantification of MOR occupancy ($n = 3$ M/2 F per condition; each point represents average total binding for one subject from 4–5 slices each). % occupancy = 100-(avg/saline avg)*100. **F** Stability of oliceridine in Phase I metabolism in rat or human liver microsomes fortified with NADPH compared to negative control without NADPH. **G** [³H]Oliceridine competition binding curve of oliceridine and metabolite TRV0109662. All values represent mean ± SEM. **H** Oliceridine major (Oxy-oliceridine) and minor (TRV0109662) metabolite molecular diagram.
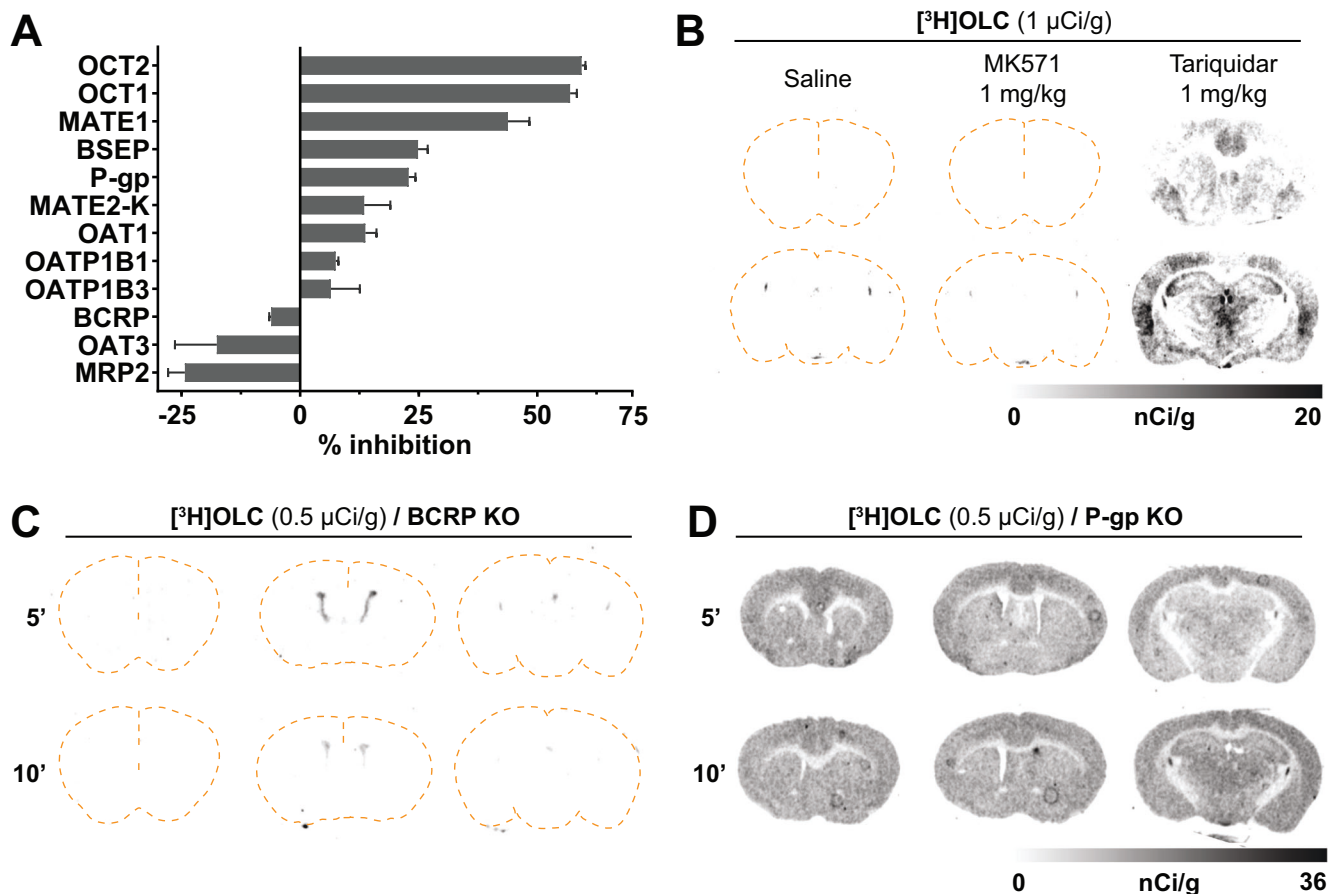

Fig. 4 Oliceridine's brain uptake is determined by its interaction with P-glycoprotein. A In vitro efflux transporter profiling of oliceridine in Caco-2 cells. Data are mean ± SEM of duplicate experiment. **B** Ex vivo brain uptake of [³H]oliceridine (OLC) (1µCi/g, i.v.) in rats co-injected with tariquidar (1 mg/kg, i.v.), MK571 (1 mg/kg, i.v.), or saline 15-min post-injection ($n = 1$/condition). Ex vivo brain uptake of [³H]oliceridine (0.5 µCi/g, i.p.) in mice with germline deletion of BCRP (**C**) or P-gp (**D**) at either 5- or 15-min post-injection ($n = 1$/condition). Dashed lines delineate brain slice outline.

major substrate (>50% inhibition) for the efflux transporters OCT1, OCT2, MATE1, and a minor substrate (>20% inhibition) for BSEP and MDR1 (P-glycoprotein, P-gp) (Fig. 4A). These transporters — with the exception of P-gp— are not expressed in the brain's endothelial compartment [34–36] and therefore we focused our subsequent efforts on interactions between oliceridine and P-gp.

We pretreated rats with either saline, tariquidar (P-gp inhibitor [37], 1 mg/kg, i.v.), or MK571 (an MRP1 inhibitor [38], 1 mg/kg, i.v.) as a negative control, followed by [³H]oliceridine (1 µCi/g, i.v.). Rats were euthanized 15-min later, and brains were harvested, sectioned, and imaged using phosphorimaging. MK571-pretreated rats showed exclusive [³H]oliceridine accumulation in the ventricles/CSF compartment (Fig. 4B) similar to rats pretreated with saline. Rats pretreated with tariquidar showed [³H]oliceridine brain uptake, including in MOR-rich regions [39]. Tariquidar inhibits P-gp but also acts as a substrate for BCRP [40]. To

examine effects of tariquidar on BCRP-mediated uptake of [³H] oliceridine, we performed [³H]oliceridine uptake experiments in MDR1 (P-gp) and BCRP knockout (KO) mice. Mice were injected with [³H]oliceridine (5 µCi/g, i.v.) and euthanized 5 or 15 min later. Their brains were harvested, sectioned, and imaged using a phosphorimager. P-gp/BCRP KO mice showed greater [³H] oliceridine brain uptake compared to BCRP KO mice, whose [³H] oliceridine brain distribution was indistinguishable from WT mice (Fig. 4C, D), confirming that oliceridine's interaction with P-gp, but not BCRP, mediates its rapid but limited brain uptake.

P-glycoprotein is a critical determinant of oliceridine's in vivo efficacy and adverse effects
To assess the implications of P-gp function on oliceridine's in vivo efficacy and adverse effect profile, we examined oliceridine's analgesic (hot plate antinociception), respiratory depressive

(blood oxygen saturation), and abuse liability (intravenous self-administration) effects using WT and P-gp/BCRP KO rats.

Antinociception. First, we assessed the in vivo antinociceptive efficacy of oliceridine and compared it to morphine using the hot plate ($n = 2$–3 M/3 F per genotype per drug, $n = 22$ total) (Fig. 5A, B). We chose doses previously shown to produce moderate levels of antinociception in rodents in this procedure [5, 27]. Latency for nociceptive behavioral responding was recorded at multiple time points directly before and following morphine (10 mg/kg, s.c.) or oliceridine (0.3 mg/kg, s.c.) exposure in both KO and WT rats. Changes in nociceptive responses to morphine (10 mg/kg, s.c.) or oliceridine (0.3 mg/kg, s.c.) were consistent with previous reports [5, 12, 13, 27]. The three-way mixed-model analysis of opioid-induced thermal antinociception (%MPE), showed significant main effects of time (F (2.633, 46.34) = 30.6, $p < 0.001$), drug (F (1, 18) = 8.917, $p < 0.01$), genotype (F (1, 18) = 119.9, $p < 0.001$); as well as the time x drug x genotype interaction (F (5, 88) = 11.94, $p < 0.001$). A Tukey post hoc analysis revealed that morphine antinociceptive efficacy in KO rats peaked between 60- ($p < 0.001$) and 120-min ($p < 0.001$) after injection. In contrast, oliceridine demonstrated a more rapid onset of antinociception that peaked 15 min ($p < 0.001$) post-injection that was followed by a quick decay, with oliceridine-treated rats returning to baseline by 120 min post-injection.

Respiratory depression. To determine the effect of P-gp on oliceridine- and morphine-induced respiratory depression, we measured blood oxygen saturation in awake, unrestrained WT and KO rats using pulse oximetry ($n = 2$–3 M/3 F per genotype per drug, $n = 22$ total) (Fig. 5C, D). Baseline oxygen saturation (spO_2) was measured 15 min prior to either morphine (10 mg/kg, s.c.) or oliceridine (0.3 mg/kg, s.c.) administration and across a timeseries thereafter. The three-way mixed-model analysis of opioid-induced respiratory depression (%spO2 from baseline) showed significant main effects of genotype (F(1, 20) = 56.84, $p < 0.001$), time (F(5, 82) = 9.13, $p < 0.001$), and interactions of time x drug x genotype (F (5, 82) = 12.47, $p < 0.001$). A Tukey post hoc analysis revealed that both oliceridine and morphine at these doses induced statistically comparable reductions in blood oxygen concentration in KO rats but failed to produce significant alterations from baseline in their WT counterparts. In morphine-treated KO rats, spO_2 dropped significantly at 30 min ($p < 0.001$) and peaked 60 min ($p < 0.001$) post-injection. In contrast, oliceridine-induced respiratory effects peaked 15 min ($p < 0.001$) post-injection, consistent with its faster pharmacokinetics and the time course of its antinociceptive effects. Furthermore, oliceridine's effect on spO_2 was also more short-lived than morphine's, having returned to baseline levels by 60-min post injection, whereas morphine had a sustained effect on spO_2, persisting up to 120-min ($p = 0.018$) post-injection.

Intravenous self-administration. Rodent operant self-administration paradigms are frequently performed to assess a drug's reinforcing effects and to predict its potential for abuse. Previous studies demonstrated that oliceridine is self-administered in rats previously trained to self-administer oxycodone [15], but it is unknown whether rats can acquire oliceridine self-administration. Unlike drug substitution paradigms, the predictive validity of drug self-administration acquisition studies are not influenced by the effects of prior drug exposure and are therefore more strict in assessing a drugs' reinforcing efficacy [41]. Moreover, to our knowledge, the effect of P-gp/BCRP deletion on opioid self-administration has not been previously reported. To examine this, we first trained WT and KO rats ($n = 4$ F KO, 5 F WT) to lever press for sucrose pellets on a FR1 schedule for four days (Fig. S2A–C). The two-way repeated measures (RM) ANOVA of the number of sucrose rewards earned per day showed significant

main effects of session (F(1.442, 10.09) = 16.38, $p = 0.001$). No significant differences were found between genotypes across sessions (F(1, 7) = 1.74, $p > 0.5$).

Next, subjects were trained to self-administer oliceridine across escalating doses for 15 days using FR1 and FR3 schedules (Fig. 5E). The two-way ANOVA of the number of infusions per day showed significant main effects of genotype (F(1, 7) = 19.96, $p = 0.0029$), session (F(14, 98) = 4.94, $p < 0.001$), and interaction (F(14, 98) = 4.175, $p < 0.001$). Once all WT rats' self-administration met criteria, we analyzed the preference for the active versus inactive lever to evaluate possible nonspecific responding (Fig. 5F). The mixed-model analysis of the number of responses committed over three sequential sessions showed significant effects of genotype (F (1, 10) = 25.32, $p < 0.001$), lever (F (1, 4) = 76.72, $p < 0.001$) and interaction (F (1, 4) = 125.9, $p < 0.001$). Notably, KO rats did not meet learning criteria for self-administration.

We hypothesized that the lack of discriminative responding in KO rats was driven by increased oliceridine potency due to greater brain drug exposure. To test this, we performed a dose-response assessment in both the WT and KO rats (Fig. 5G–I). The two-way RM ANOVA of the number of infusions per day showed significant main effects of genotype (F(1, 7) = 25.89, $p = 0.0014$), dose (F(5, 35) = 4.25, $p = 0.004$), and interaction (F(5, 35) = 7.22, $p < 0.001$). In a follow-up Holm-Sidak post hoc comparison, KO rats demonstrated dose-dependent alterations in self-administration of oliceridine, with their pressing peaking at the 1 µg/kg unit dose with an average of 19 ± 5 infusions (Fig. 5G). In contrast, WT rats showed peak responding at a 30 µg/kg/infusion unit dose with an average of 59 ± 12 infusions. These results suggest that P-gp functional loss shifts the oliceridine intravenous self-administration unit dose-response curve to the left and down, indicating increased potency of oliceridine due to P-gp deletion.

Following dose-response testing, WT rats were tested for extinction of goal-directed pressing. Rats were returned to 300 µg/kg/inf FR3 for one session followed by 4 consecutive days of saline self-administration (Fig. S2E). The one-way RM ANOVA of the number of infusions earned across sessions showed significant effects of session (F (6, 24) = 10.55, $p < 0.001$). In Holm-Sidak post hoc comparisons, rat active lever presses steadily diminished across each session and plateaued at 12 ± 10 infusions. Next, WT rats were tested for drug-induced reinstatement. An injection of oliceridine (0.3 mg/kg, s.c.) was administered at the start of the final saline self-administration session. All rats demonstrated a significant increase in active lever pressing from that of the final extinction trial ($p < 0.001$), indicating drug-induced reinstatement of drug-reward seeking behavior.

DISCUSSION

The primary aim of our study was to understand the pharmacodynamic and pharmacokinetic mechanisms by which oliceridine's in vivo potency is determined so as to inform the ongoing debate on therapeutic indices of opioid pharmaceuticals. Functional selectivity (i.e., biased signaling) is dependent on the cellular context and determined by availability of signaling effectors [42] and experimental conditions. Hence, experiments relying on overexpression of receptors in heterologous expression systems may not necessarily serve as accurate predictors of drug-receptor interactions under physiological conditions or in postmortem tissue. Our results using HEK-293 cells transiently transfected with opioid receptors agree with previous reports [13] showing that oliceridine behaves as a partial agonist for MOR (with negligible recruitment of β-arrestins) and, at higher concentrations, behaves as a full agonist of KOR (with over ~200-fold less potency compared with MOR) and has no detectable activity on DOR. In contrast to heterologous systems, GTPγS recruitment has historically been utilized to assess a ligand's efficacy for G-protein stimulation in situ in postmortem tissues [43–45]. Interestingly, we
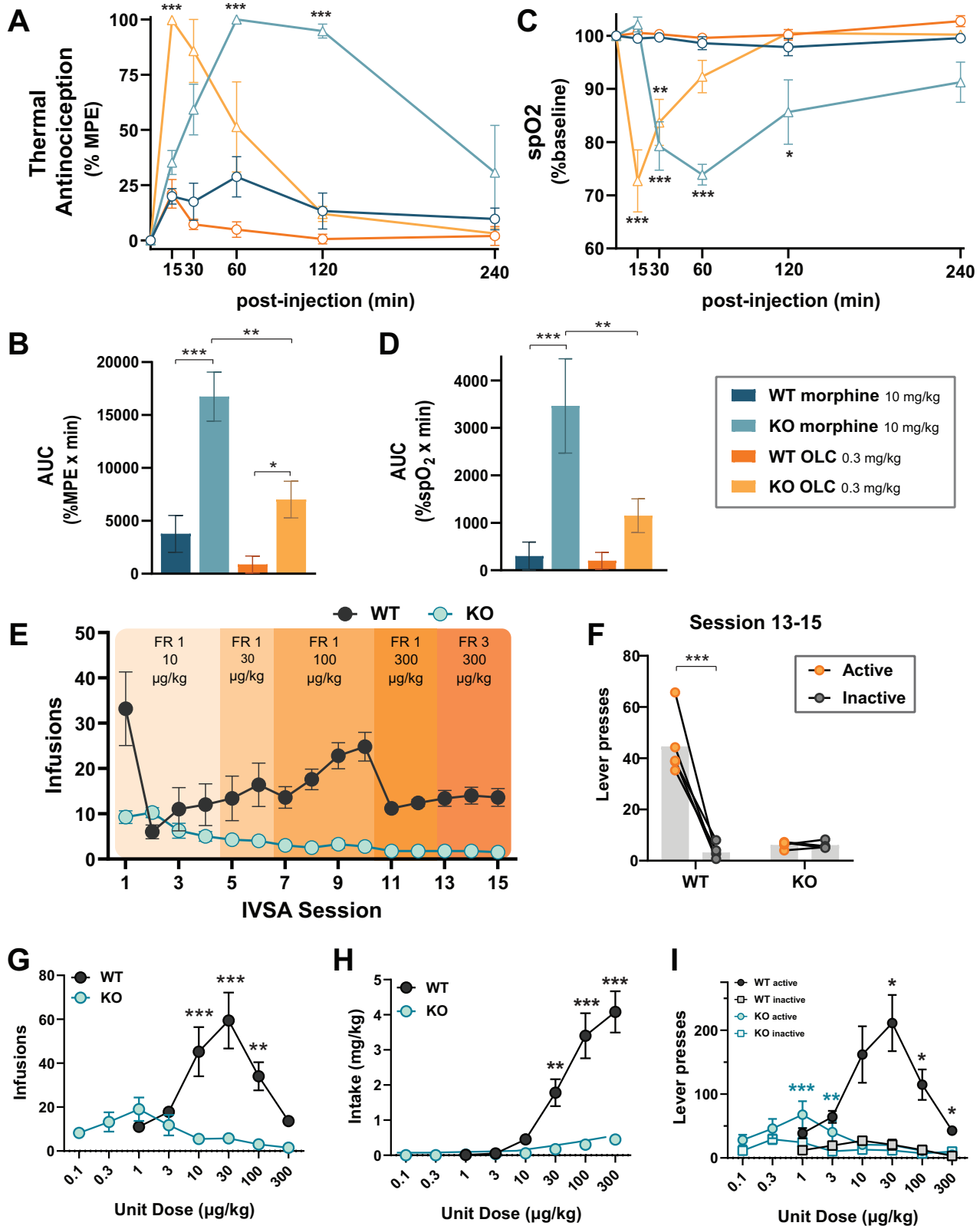
Fig. 5 P-glycoprotein is a critical determinant of oliceridine's efficacy and adverse effects. Comparison of (**A**, **B**) hotplate thermal nociception and (**C**, **D**) oxygen saturation in unrestrained rats in response to morphine (10 mg/kg, s.c.) or oliceridine (0.3 mg/kg, s.c.) between rats with germline deletion of P-gp and wild-type (WT) ($n = 4$–6/sex/condition). **E** Training data from rat i.v. selfadministration of oliceridine in WT and P-gp/BCRP KO rats ($n = 5$ F WT, 4 F KO) across increasing dose per infusion and fixed-ratio schedules. **F** Comparison between active and inactive lever presses from sessions 13–15 when responding was stable. **G**–**I** Self-administration dose response curves for i.v. oliceridine, assessing the difference in the number of infusions (**G**), total intake (**H**), and lever presses (**I**) across sessions. All data are mean ± SEM. *$p < 0.05$, **$p > 0.01$, ***$p > 0.001$.

found that oliceridine failed to stimulate [^{35}S]GTPγS recruitment in both rat brain membranes and rat brain tissue sections containing regions with high MOR density. Similar findings were recently reported by Stahl et al using membranes prepared from mouse brainstem [25]. These results contrast with the experimental findings using cell culture. This discrepancy may be due to different efficacy requirements and a lower sensitivity of the [^{35}S] GTPγS recruitment assay exacerbated by the lower density of both receptors and G proteins, as compared to transfected cultured cells. In any case, these results support the notion that oliceridine displays weak intrinsic efficacy to activate brain MOR receptors.

One hallmark of oliceridine's effects is its fast kinetics and low off-target effects [5]. Oliceridine's high potency and low efficacy might partially explain this profile, as relatively low doses are needed to achieve analgesic efficacy, favoring relatively fast clearance and allowing "safer" redosing. We also found that oliceridine has no significantly bioactive metabolites. Oliceridine's lack of pharmacologically active metabolites is possibly another important contributing factor to its favorable pharmacokinetics. This is in contrast to morphine, whose active metabolite morphine-6-glucuronide is partially responsible for the prolonged depressive effects morphine induces on respiration, which can result in a dangerous and unfavorable amplification effect on opioid-induced respiratory depression following redosing [46, 47].

Furthermore, oliceridine's low brain accumulation might favor engagement of peripheral vs. central MORs, thereby contributing to less adverse effects and a more favorable pharmacodynamic profile. Indeed, we found that oliceridine is a substrate for the P-gp efflux transporter and showed that this interaction mediates oliceridine's in vivo brain exposure, efficacy, and adverse effect profiles. Specifically, we found that manipulations leading to a loss of P-gp function dramatically increased oliceridine's brain exposure, it's antinociceptive efficacy, and its ability to induce respiratory depression and reinforcement. These observations are consistent with prior preclinical reports of other opioids (including morphine and fentanyl), whose brain exposure is modulated by P-gp [48–57]. The low doses required to achieve analgesic potency using oliceridine, coupled with its weak intrinsic efficacy as compared to morphine and fentanyl, might explain oliceridine's therapeutic index. In other words, even though morphine is also a P-gp substrate, the doses of morphine used are at least 10-fold higher than oliceridine doses and may potentially saturate efflux transporters, thereby decreasing morphine clearance and leading to higher relative brain uptake. Thus, oliceridine's saturable interaction with efflux pumps in conjunction with its relatively low intrinsic efficacy could at least partially explain oliceridine's reportedly lower adverse effect profile.

The reinforcing effects of oliceridine in either humans or in animal laboratory models are not well understood. The intravenous drug self-administration procedure is the gold standard behavioral procedure for assessing the potential abuse liability of a drug [41, 58]. To our knowledge, the ability of oliceridine to be self-administered has only been tested in rats previously trained to self-administer oxycodone [15, 16]. Here, we showed that rats can be trained to self-administer oliceridine without prior exposure to other opioids/drugs. In addition, WT rats trained to self-administer oliceridine showed extinction and drug-induced reinstatement comparable with other opioids [59–61]. Interestingly, we found that rats that lack P-gp did not meet discrimination criteria for oliceridine self-administration during training. For this reason, we were unable to test KO rats on extinction and reinstatement, and therefore we cannot make any conclusions as to whether P-gp regulates such behaviors. However, KO rats demonstrated canonical inverted U-shaped dose-dependent responding at markedly lower unit doses of oliceridine. The seemingly counterintuitive finding that KO rats did not show high lever pressing during the self-administration training period might be due to the slower clearance of oliceridine in these rats—as seen in the longer

duration of action in KO rats during the hot plate antinociception assay compared to their WT littermates and as supported by the [^{3}H]oliceridine biodistribution findings. This may have created a confounding factor for the rats to associate the drug effects with their associated cues (as described in some studies [62–64] but not others [65, 66]). Another explanation may be that the brain concentration of oliceridine achieved in P-gp/BCRP KO rats might be too high and no longer reinforcing or may have been sufficient to induce partial sedation. In fact, in a dose response experiment, P-gp/BCRP KO rats had a peak response to oliceridine when infused at 1 μg/kg/inf, a unit dose 30-fold lower than the peak dose for WT rats. Overall, these results indicate that P-gp function is a key factor that determines the reinforcing properties of opioids, and that genetic or environmental factors (e.g., diet, other drug/medication exposure [67–69]) affecting P-gp function should be considered when evaluating the abuse liability of opioids.

In sum, our results support the purported functional selectivity of oliceridine being attributable to low intrinsic efficacy at MOR and demonstrate a significant impact of P-gp on the pharmacokinetic, pharmacodynamic, and efficacy profiles of oliceridine. P-gp (and other efflux pumps [70–72]) are known modulators of opiate potency in the clinic and, as we show here, a key determinant of their abuse liability. Consequently, our findings suggest that P-gp function be considered when prescribing oliceridine to patients and evaluating their therapeutic outcome.

REFERENCES

1. Stanczyk MA, Kandasamy R. Biased agonism: the quest for the analgesic holy grail. Pain Rep. 2018;3:e650.
2. Bohn LM, Gainetdinov RR, Lin FT, Lefkowitz RJ, Caron MG. Mu-opioid receptor desensitization by beta-arrestin-2 determines morphine tolerance but not dependence. Nature. 2000;408:720–3.
3. Raehal KM, Walker JKL, Bohn LM. Morphine side effects in beta-arrestin 2 knockout mice. J Pharmacol Exp Ther. 2005;314:1195–201.
4. Bohn LM, Lefkowitz RJ, Gainetdinov RR, Peppel K, Caron MG, Lin FT. Enhanced morphine analgesia in mice lacking beta-arrestin 2. Science. 1999;286:2495–8.
5. DeWire SM, Yamashita DS, Rominger DH, Liu G, Cowan CL, Graczyk TM, et al. A G protein-biased ligand at the μ-opioid receptor is potently analgesic with reduced gastrointestinal and respiratory dysfunction compared with morphine. J Pharmacol Exp Ther. 2013;344:708–17.
6. Montandon G, Ren J, Victoria NC, Liu H, Wickman K, Greer JJ, et al. G-protein-gated inwardly rectifying potassium channels modulate respiratory depression by opioids. Anesthesiology. 2016;124:641–50.
7. Kliewer A, Gillis A, Hill R, Schmiedel F, Bailey C, Kelly E, et al. Morphine-induced respiratory depression is independent of β-arrestin2 signalling. Br J Pharmacol. 2020;177:2923–31.
8. Azevedo Neto, J, Costanzini A, De Giorgio R, Lambert DG, Ruzza C, Calò G. Biased versus partial agonism in the search for safer opioid analgesics. Molecules. 2020;25:3870
9. Kliewer A, Schmiedel F, Sianati S, Bailey A, Bateman JT, Levitt ES, et al. Phosphorylation-deficient G-protein-biased μ-opioid receptors improve analgesia and diminish tolerance but worsen opioid side effects. Nat Commun. 2019;10:367.
10. Soergel DG, Subach RA, Burnham N, Lark MW, James IE, Sadler BM, et al. Biased agonism of the μ-opioid receptor by TRV130 increases analgesia and reduces on-target adverse effects versus morphine: A randomized, doubleblind, placebo-controlled, crossover study in healthy volunteers. Pain. 2014;155:1829–35.
11. Singla NK, Skobieranda F, Soergel DG, Salamea M, Burt DA, Demitrack MA, et al. APOLLO-2: a randomized, placebo and active-controlled phase III study investigating oliceridine (TRV130), a G protein-biased ligand at the μ-opioid receptor, for management of moderate to severe acute pain following abdominoplasty. Pain Pract. 2019;19:715–31.
12. Manglik A, Lin H, Aryal DK, McCorvy JD, Dengler D, Corder G, et al. Structure-based discovery of opioid analgesics with reduced side effects. Nature. 2016;537:185–90.
13. Gillis A, Gondin AB, Kliewer A, Sanchez J, Lim HD, Alamein C, et al. Low intrinsic efficacy for G protein activation can explain the improved side effect profiles of new opioid agonists. Sci Signal. 2020;13:eaaz3140.
14. Altarifi AA, David B, Muchhala KH, Blough BE, Akbarali H, Negus SS. Effects of acute and repeated treatment with the biased mu opioid receptor agonist TRV130 (oliceridine) on measures of antinociception, gastrointestinal function, and abuse liability in rodents. J Psychopharmacol (Oxford). 2017;31:730–9.

15. Austin Zamarripa C, Edwards SR, Qureshi HN, Yi JN, Blough BE, Freeman KB. The G-protein biased mu-opioid agonist, TRV130, produces reinforcing and anti-nociceptive effects that are comparable to oxycodone in rats. Drug Alcohol Depend. 2018;192:158–62.

16. Bossert JM, Kiyatkin EA, Korah H, Hoots JK, Afzal A, Perekopskiy D. et al. In a rat model of opioid maintenance, the G protein-biased mu opioid receptor agonist TRV130 decreases relapse to oxycodone seeking and taking and prevents oxycodone-induced brain hypoxia. Biol. Psychiatry. 2020;88:935–44.

17. Townsend EA, Blough BE, Epstein DH, Negus SS, Shaham Y, Banks ML. Effect of TRV130 and methadone on fentanyl-vs.-food choice and somatic withdrawal signs in opioid-dependent and post-opioid-dependent rats. Neuropsychopharmacology. 2022;47:2132–9. https://doi.org/10.1038/s41386-022-01393-3.

18. Ohta Y, Furuta T, Nagai T, Horikawa K. Red fluorescent cAMP indicator with increased affinity and expanded dynamic range. Sci Rep 2018;8:1866.

19. Bonaventura J, Eldridge M, Hu F, Gomez JL, Sanchez-Soto M, Abramyan AM, et al. High-potency ligands for DREADD imaging and activation in rodents and monkeys. Nat Commun 2019;10:4627.

20. Marchette RCN, Gregory-Flores A, Tunstall BJ, Carlson ER, Jackson SN, Sulima A, et al. κ-Opioid receptor antagonism reverses heroin withdrawalinduced hyperalgesia in male and female rats. Neurobiol Stress. 2021;14:100325.

21. Fredriksson I, Applebey SV, Minier-Toribio A, Shekara A, Bossert JM, Shaham Y. Effect of the dopamine stabilizer (-)-OSU6162 on potentiated incubation of opioid craving after electric barrier-induced voluntary abstinence. Neuropsychopharmacology. 2020;45:770–9.

22. Bonaventura J, S Lam, M Carlton, MA Boehm, JL Gomez, O Solís, et al. Pharmacological and behavioral divergence of ketamine enantiomers:implications for abuse liability. Mol Psychiatry. 2021. https://doi.org/10.1038/s41380021-01093-2

23. Pedersen MF, Wróbel TM, Märcher-Rørsted E, Pedersen DS, Møller TC, Gabriele F, et al. Biased agonism of clinically approved μ-opioid receptor agonists and TRV130 is not controlled by binding and signaling kinetics. Neuropharmacology. 2020;166:107718.

24. Chen X-T, Pitis P, Liu G, Yuan C, Gotchev D, Cowan CL. et al. Structure–Activity Relationships and Discovery of a G Protein Biased μ Opioid Receptor Ligand, [(3-Methoxythiophen-2-yl)methyl]({2-[(9R)-9-(pyridin-2-yl)-6-oxaspiro[4.5]decan-9-yl]ethyl})amine (TRV130), for the Treatment of Acute Severe Pain. J Med Chem. 2013;56:8019–31.

25. Stahl EL, Schmid CL, Acevedo-Canabal A, Read C, Grim TW, Kennedy NM, et al. G protein signaling-biased mu opioid receptor agonists that produce sustained G protein activation are noncompetitive agonists. Proc Natl Acad Sci USA. 2021;118:e2102178118.

26. Zhang X, Hutchins SD, Blough BE, Vallender EJ. In vitro effects of ligand bias on primate mu opioid receptor downstream signaling. Int J Mol Sci. 2020;21:3999.

27. Yang Y, Wang Y, Zuo A, Li C, Wang W, Jiang W, et al. Synthesis, biological, and structural explorations of a series of μ-opioid receptor (MOR) agonists with high G protein signaling bias. Eur J Med Chem. 2022;228:113986.

28. Stott LA, Hall DA, Holliday ND. Unravelling intrinsic efficacy and ligand bias at G protein coupled receptors: A practical guide to assessing functional data. Biochem Pharmacol. 2016;101:1–12.

29. Kelly E. Efficacy and ligand bias at the μ-opioid receptor. Br J Pharmacol. 2013;169:1430–46.

30. U.S. Food and Drug Administration Advisory Committee. *FDA advisory committee briefing document: Oliceridine, meeting of the anesthetic and analgesic drug products advisory committee.* (2018).

31. Nafziger AN, Arscott KA, Cochrane K, Skobieranda F, Burt DA, Fossler MJ. The influence of renal or hepatic impairment on the pharmacokinetics, safety, and tolerability of oliceridine. Clin Pharmacol Drug Dev. 2020;9:639–50.

32. Dagenais C, Graff CL, Pollack GM. Variable modulation of opioid brain uptake by P-glycoprotein in mice. Biochem Pharmacol. 2004;67:269–76.

33. Callaghan R, Riordan JR. Synthetic and natural opiates interact with P-glycoprotein in multidrug-resistant cells. J Biol Chem. 1993;268:16059–64.

34. Okura T, Ito R, Ishiguro N, Tamai I, Deguchi Y. Blood-brain barrier transport of pramipexole, a dopamine D2 agonist. Life Sci. 2007;80:1564–71.

35. Lickteig AJ, Cheng X, Augustine LM, Klaassen CD, Cherrington NJ. Tissue distribution, ontogeny and induction of the transporters Multidrug and toxin extrusion (MATE) 1 and MATE2 mRNA expression levels in mice. Life Sci. 2008;83:59–64.

36. Alnouti Y, Petrick JS, Klaassen CD. Tissue distribution and ontogeny of organic cation transporters in mice. Drug Metab Dispos. 2006;34:477–82.

37. Weidner LD, Fung KL, Kannan P, Moen JK, Kumar JS, Mulder J, et al. Tariquidar is an inhibitor and not a substrate of human and mouse pglycoprotein. Drug Metab Dispos. 2016;44:275–82.

38. Mease K, Sane R, Podila L, Taub ME. Differential selectivity of efflux transporter inhibitors in Caco-2 and MDCK-MDR1 monolayers: a strategy to assess the interaction of a new chemical entity with P-gp, BCRP, and MRP2. J Pharm Sci. 2012;101:1888–97.

39. Mansour A, Fox CA, Thompson RC, Akil H, Watson S. J. mu-Opioid receptor mRNA expression in the rat CNS: comparison to mu-receptor binding. Brain Res. 1994;643:245–65.

40. Kannan P, Telu S, Shukla S, Ambudkar SV, Pike VW, Halldin C, et al. The "specific" P-glycoprotein inhibitor Tariquidar is also a substrate and an inhibitor for breast cancer resistance protein (BCRP/ABCG2). ACS Chem Neurosci. 2011;2:82–9.

41. O'Connor EC, Chapman K, Butler P, Mead AN. The predictive validity of the rat self-administration model for abuse liability. Neurosci Biobehav Rev. 2011;35:912–38.

42. Seyedabadi M, Ghahremani MH, Albert PR. Biased signaling of G protein coupled receptors (GPCRs): Molecular determinants of GPCR/transducer selectivity and therapeutic potential. Pharmacol Ther. 2019;200:148–78.

43. Burkey TH, Ehlert FJ, Hosohata Y, Quock RM, Cowell S, Hosohata K, et al. The efficacy of δ-opioid receptor-selective drugs. Life Sci. 1998;62:1531–6.

44. Sim LJ, Selley DE, Xiao R, Childers SR. Differences in G-protein activation by μ- and δ-opioid, and cannabinoid, receptors in rat striatum. Eur J Pharmacol. 1996;307:97–105.

45. Selley DE, Liu Q, Childers SR. Signal transduction correlates of mu opioid agonist intrinsic efficacy: receptor-stimulated [35S]GTP gamma S binding in mMOR-CHO cells and rat thalamus. J Pharmacol Exp Ther. 1998;285:496–505.

46. Gong QL, Hedner T, Hedner J, Björkman R, Nordberg G. Antinociceptive and ventilatory effects of the morphine metabolites: morphine-6-glucuronide and morphine-3glucuronide. Eur J Pharmacol. 1991;193:47–56.

47. Romberg R, Sarton E, Teppema L, Matthes HW, Kieffer BL, Dahan A. Comparison of morphine-6-glucuronide and morphine on respiratory depressant and anti-nociceptive responses in wild type and mu-opioid receptor deficient mice. Br J Anaesth. 2003;91:862–70.

48. Letrent SP, Pollack GM, Brouwer KR, Brouwer KL. Effects of a potent and specific P-glycoprotein inhibitor on the blood-brain barrier distribution and anti-nociceptive effect of morphine in the rat. Drug Metab Dispos. 1999;27:827–34.

49. Thompson SJ, Koszdin K, Bernards CM. Opiate-induced analgesia is increased and prolonged in mice lacking P-glycoprotein. Anesthesiology. 2000;92:1392–9.

50. Zong J, Pollack GM. Morphine antinociception is enhanced in mdr1a gene-deficient mice. Pharm Res. 2000;17:749–53.

51. Shimizu N, Kishioka S, Maeda T, Fukazawa Y, Yamamoto C, Ozaki M, et al. Role of pharmacokinetic effects in the potentiation of morphine analgesia by L-Type calcium channel blockers in mice. J Pharmacol Sci. 2004;94:240–5.

52. Hamabe W, Maeda T, Fukazawa Y, Kumamoto K, Shang LQ, Yamamoto A, et al. P-glycoprotein ATPase activating effect of opioid analgesics and their Pglycoprotein-dependent antinociception in mice. Pharmacol Biochem Behav. 2006;85:629–36.

53. King M, Su W, Chang A, Zuckerman A, Pasternak GW. Transport of opioids from the brain to the periphery by P-glycoprotein: peripheral actions of central drugs. Nat Neurosci. 2001;4:268–74.

54. Liang D-Y, Liao G, Lighthall GK, Peltz G, Clark DJ. Genetic variants of the Pglycoprotein gene Abcb1b modulate opioid-induced hyperalgesia, tolerance and dependence. Pharmacogenet Genomics. 2006;16:825–35.

55. Yu C, Yuan M, Yang H, Zhuang X, Li H. P-glycoprotein on blood-brain barrier plays a vital role in fentanyl brain exposure and respiratory toxicity in rats. Toxicol Sci. 2018;164:353–62.

56. Rodriguez M, Ortega I, Soengas I, Suarez E, Lukas JC, Calvo R. Effect of P-glycoprotein inhibition on methadone analgesia and brain distribution in the rat. J Pharm Pharmacol. 2004;56:367–74.

57. Sanchez-Covarrubias L, Slosky LM, Thompson BJ, Zhang Y, Laracuente ML, DeMarco KM, et al. P-glycoprotein modulates morphine uptake into the CNS: a role for the non-steroidal anti-inflammatory drug diclofenac. PLoS One. 2014;9:e88516.

58. Carter LP, Griffiths RR. Principles of laboratory assessment of drug abuse liability and implications for clinical development. Drug Alcohol Depend. 2009;105:S14–25.

59. Ma D, Yue K, Chen L, Tian X, Ru Q, Gan Y, et al. L-stepholidine, a natural dopamine receptor D1 agonist and D2 antagonist, inhibits heroin-induced reinstatement. Neurosci Lett. 2014;559:67–71.

60. Malone SG, Keller PS, Hammerslag LR, Bardo MT. Escalation and reinstatement of fentanyl self-administration in male and female rats. Psychopharmacology. 2021;238:2261–73.

61. De Vries TJ, Schoffelmeer AN, Binnekade R, Mulder AH, Vanderschuren LJ. Drug-induced reinstatement of heroin- and cocaine-seeking behaviour following long-term extinction is associated with expression of behavioural sensitization. Eur J Neurosci. 1998;10:3565–71.

62. Liu Y, Roberts DCS, Morgan D. Sensitization of the reinforcing effects of self-administered cocaine in rats: effects of dose and intravenous injection speed. Eur J Neurosci. 2005;22:195–200.

63. Porrino LJ. Functional consequences of acute cocaine treatment depend on route of administration. Psychopharmacology. 1993;112:343–51.

64. Samaha A-N, Yau W-YW, Yang P, Robinson TE. Rapid delivery of nicotine promotes behavioral sensitization and alters its neurobiological impact. Biol Psychiatry. 2005;57:351–60.

65. Crombag HS, Ferrario CR, Robinson TE. The rate of intravenous cocaine or amphetamine delivery does not influence drug-taking and drug-seeking behavior in rats. Pharmacol Biochem Behav. 2008;90:797–804.

66. Samaha A-N, Minogianis E-A, Nachar W. Cues paired with either rapid or slower self-administered cocaine injections acquire similar conditioned rewarding properties. PLoS One. 2011;6:e26481.

67. Zhang W, Han Y, Lim SL, Lim LY. Dietary regulation of P-gp function and expression. Expert Opin Drug Metab Toxicol. 2009;5:789–801.

68. Mealey KL, Barhoumi R, Burghardt RC, Safe S, Kochevar DT. Doxycycline induces expression of P glycoprotein in MCF-7 breast carcinoma cells. Antimicrob Agents Chemother. 2002;46:755–61.

69. Wang J-S, Zhu H-J, Markowitz JS, Donovan JL, DeVane CL. Evaluation of antipsychotic drugs as inhibitors of multidrug resistance transporter P-glycoprotein. Psychopharmacology. 2006;187:415–23.

70. Venkatasubramanian R, Fukuda T, Niu J, Mizuno T, Chidambaran V, Vinks AA, et al. ABCC3 and OCT1 genotypes influence pharmacokinetics of morphine in children. Pharmacogenomics. 2014;15:1297–309.

71. Meyer MJ, Neumann VE, Friesacher HR, Zdrazil B, Brockmöller J, Tzvetkov MV. Opioids as substrates and inhibitors of the genetically highly variable 2 organic cation transporter OCT1. J Med Chem. 2019;62:9890–905.

72. Tzvetkov MV, dos Santos Pereira JN, Meineke I, Saadatmand AR, Stingl JC, Brockmöller J. Morphine is a substrate of the organic cation transporter OCT1 and polymorphisms in OCT1 gene affect morphine pharmacokinetics after codeine administration. Biochem Pharmacol. 2013;86:666–78.

COMPETING INTERESTS
MM has received research funding from AstraZeneca, Redpin Therapeutics and Attune Neurosciences. All other authors declare no conflicts of interest.

ADDITIONAL INFORMATION
Supplementary information The online version contains supplementary material available at https://doi.org/10.1038/s41386-022-01507-x.

Correspondence and requests for materials should be addressed to Jordi Bonaventura or Michael Michaelides.

Reprints and permission information is available at http://www.nature.com/reprints

Publisher's note Springer Nature remains neutral with regard to jurisdictional claims in published maps and institutional affiliations.